Advancements in Engineering Turbulence Modeling

T.-H. Shih

Center for Modeling of Turbulence and Transition

ICOMP/NASA Lewis Research Center

9th National Aero-Space Plane

Technology Symposium

November 1-2, 1990

Paper Number 105

ABSTRACT

Some new developments in two-equation models and second order closure models will be presented. Two-equation models (e.g., k-ϵ model) have been widely used in CFD for engineering problems. Most of low-Reynolds number two-equation models contain some wall-distance damping functions to acount for the effect of wall on turbulence. However, this often causes the confusions and difficulties in computing flows with complex geometry and also needs an ad hoc treatment near the separation and reattachment points. In this paper, a set of modified two-equation models is proposed to remove abovementioned shortcomings. The calculations using various two-equation models are compared with direct numerical simulations of channel flows and flat boundary layers.

Development of second order closure model will be also discussed with emphasis on the modeling of pressure related correlation terms and dissipation rates in the second moment equations. All the existing models poorly predict the normal stresses near the wall and fail to predict the 3 dimensional effect of mean flow on the turbulence (e.g., decrease in the shear stress caused by the cross flow in the boundary layer). The newly developed second order near-wall turbulence model to be described in this paper is capable of capturing the near-wall behavior of turbulence as well as the effect of three dimension mean flow on the turbulence.

1. k-ϵ model

The two-equation model, especially k-ϵ model, is still the most widely used model for computing engineering flows. We first list some of the commonly used two-equation models,[1],[2],[3],[4],[5],[6] and their predictions on the fully developed channel flows and boundary layer flows compared with the corresponding direct numerical simulations. Then, we propose a modified k-ϵ model which does not contain any wall distance. The proposed k-ϵ model has been also tested using direct numerical simulation data.

The eddy viscosity ν_T is assumed in two-equation models as follows:

$$\nu_T = C_\mu f_\mu \frac{k^2}{\tilde{\epsilon}}$$

or

$$\nu_T = C_\mu f_\mu k\tau$$

where $\tau = k^2/\tilde{\epsilon}$

The general k-ϵ (or k-τ) model equations are of the following forms:

$$k_{,t} + U_j k_{,j} = \left[\left(\frac{\nu_T}{\sigma_k} + \nu\right) k_{,j}\right]_{,j} + \Pi + \nu_T \left(U_{i,j} + U_{j,i}\right) U_{i,j} - \epsilon + D$$

$$\epsilon_{,t} + U_j \epsilon_{,j} = \left[\left(\frac{\nu_T}{\sigma_\epsilon} + \nu\right) \epsilon_{,j}\right]_{,j} + C_1 \frac{\epsilon}{k} \nu_T \left(U_{i,j} + U_{j,i}\right) U_{i,j} - C_2 f_2 \frac{\epsilon\tilde{\epsilon}}{k} + E$$

$$\tau_{,t} + U_j \tau_{,j} = \left[\left(\frac{\nu_T}{\sigma_{\tau 2}} + \nu\right) \tau_{,j}\right]_{,j} + \frac{2}{k}\left(\frac{\nu_T}{\sigma_{\tau 1}} + \nu\right) k_{,i}\tau_{,i} - \frac{2}{\tau}\left(\frac{\nu_T}{\sigma_{\tau 1}} + \nu\right) \tau_{,i}\tau_{,i}$$
$$+ (1 - C_{\epsilon 1})\frac{\tau}{k}\nu_T (U_{i,j} + U_{j,i}) U_{i,j} + (C_{\epsilon 2} f_2 - 1)$$

This table lists the model terms, damping functions and model constants appeared in various two-equation models

$Model$	E	$\vec{\epsilon}$	C_1	C_2	f_1	f_2
JL	$2\nu\nu_t(\frac{\partial^2 u}{\partial y^2})^2$	ϵ	1.45	2.0	1.0	$1-.3e^{(-R_t^2)}$
LB	0	ϵ	1.44	2.0	$1+(\frac{.05}{f_\mu})^2$	$1-e^{(-R_t^2)}$
$Chien$	$\frac{-2\nu\epsilon}{y^2}$	ϵ	1.35	1.8	1.0	$1-.22e^{(-R_t^2/36)}$
NH	$\nu\nu_t(1-f_\mu)(\frac{\partial^2 u}{\partial y^2})^2$	ϵ	1.45	1.9	1.0	$1-.3e^{(-R_t^2)}$
$Shih$	$\nu\nu_t(\frac{\partial^2 u}{\partial y^2})^2$	$\epsilon-\frac{\nu}{2k}(\frac{\partial k}{\partial x_i})^2$	1.45	2.0	1.0	$1-.22e^{(-R_t^2/36)}$

$Model$	Π	D	f_μ	σ_k
JL	0	$-2\nu(\frac{\partial\sqrt{k}}{\partial y})^2$	$e^{(\frac{-2.5}{1+R_t/50})}$	1.0
LB	0	0	$[1-e^{(-.0165R_k)}]^2(1+\frac{20.5}{R_t})$	1.0
$Chien$	0	$-2\nu k/y^2$	$1-e^{(-.0155y^+)}$	1.0
NH	0	$-2\nu(\frac{\partial\sqrt{k}}{\partial y})^2$	$[1-e^{(-y^+/26.5)}]^2$	1.0
SAA	0	0	$(1+\frac{3.45}{\sqrt{Re_t}})tanh(\frac{y^+}{70})$	1.36
$Shih$	$\frac{.05\nu_t k_{,ii}}{\sigma_k f_\mu[1-exp(-y^+)]}$	0	$1-e^{(-6\times10^{-3}y^+-4\times10^{-4}y^{+2}+2.5\times10^{-6}y^{+3}-4\times10^{-9}y^{+4})}$	1.3

$$\nu_t = C_\mu f_\mu \frac{k^2}{\tilde{\epsilon}} \qquad y^+ = \frac{u_\tau y}{\nu} \qquad R_t = \frac{k^2}{\nu\epsilon} \qquad R_k = \frac{\sqrt{k}y}{\nu}$$

The following figures show the predictions on fully develop channel flow using various two-equation models compared with the direct numerical simulation data.[7] Ploted quantities include the mean velocity U, turbulent shear stress $\langle uv \rangle$, turbulent kinetic energy k and dissipation rate EPS ϵ. The open circle represents direct numerical simulation, and the solid line represents the model prediction.

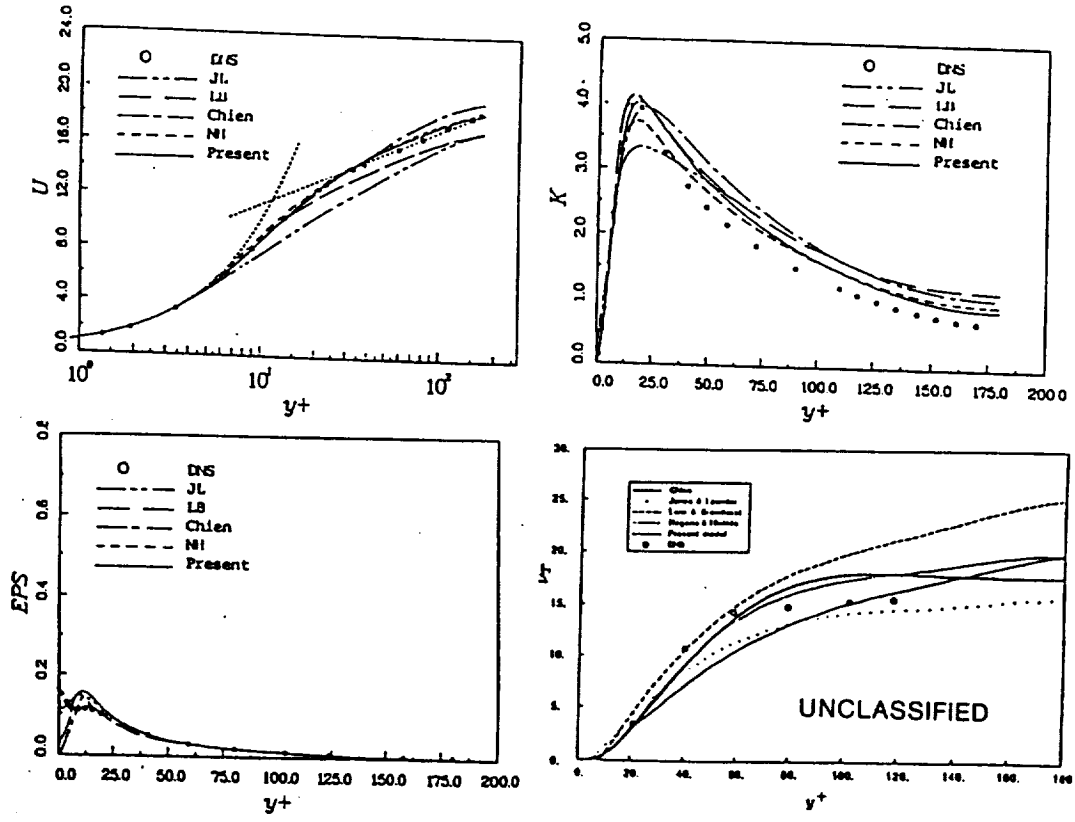

The figures below show the model predictions on flat plate boundary layer flow. A direct numerical simulation of boundary layer flow[8] is used for comparison. The skin friction coefficient C_f is also included in the comparisons.

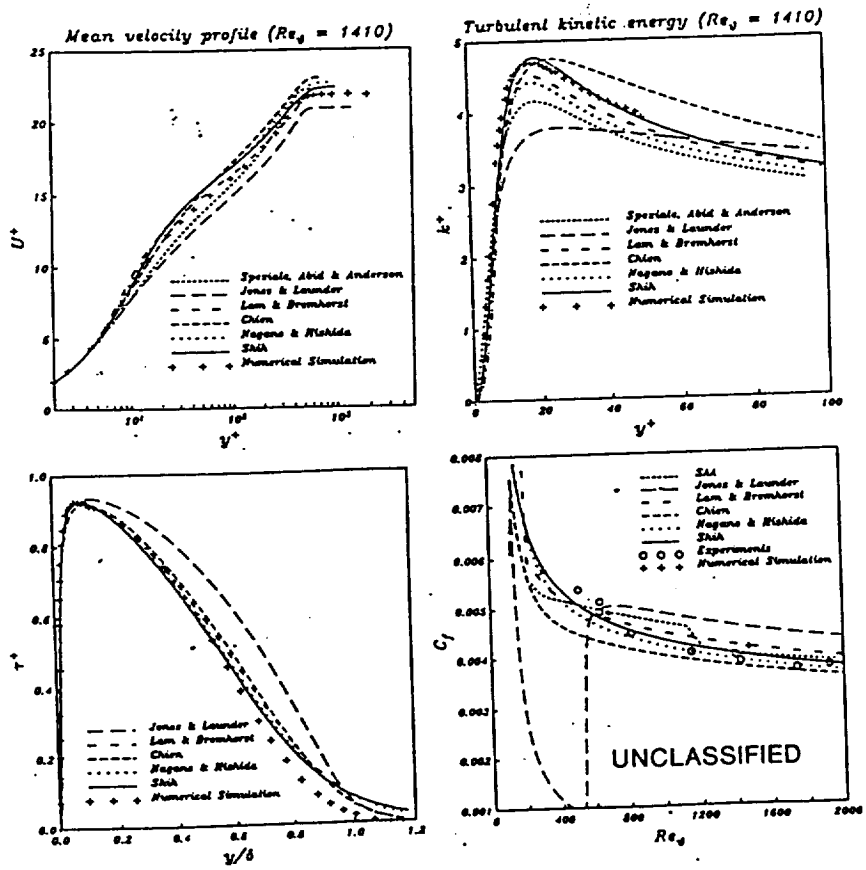

Overall, Shih's k-ϵ model gives better prediction in both fully developed channel flows and flat plate boundary layer flows according to the comparisons with corresponding direct numerical simulations. However, this model has the same problem as the others, that is it contains the wall distance parameter y^+, which is defined as

$$y^+ = \frac{u_\tau y}{\nu}$$

where u_τ is the friction velocity. The difficulty would occure in some situations. For example, near the seperation point u_τ aproaches zero and hence ν_t (through $f_\mu(y^+)$) will approach zero everywhere when this u_τ is used. Another example is the flow with complex geometry that the wall distance is not well defined. In the both cases, the ad hoc treatment is needed in the model implimentation. We notice that Jonse-Launder's model[1] does not contain y^+. However, its present form does not perform very well in the simple testing flows. Here, we based on the Shih's k-ϵ model modify the parts which is related the y^+ with another parameter $R = \frac{k^{3/2}}{\epsilon}\frac{|U|}{\nu}$. R is a ratio of turbulence length scale to viscous length scale. The modifications[9] made here are:

$$f_\mu = 1 - \exp\left\{C_3\left[1 - \exp(C_6 R^{1/4})\right]\right\}$$

$$\Pi = \left[\frac{C_0}{f_\mu^2}\frac{\nu_T}{\sigma_k}k_{,j}\right]_{,j}$$

$$\tilde{\epsilon} = \epsilon\left[1 - \exp(-R_t^{1/2})\right]$$

where $R_t = k^2/\nu\epsilon$, $C_0 = .004$, $C_3 = .0004$, $C_6 = 1.2$

The following figures show the predictions from the present model on fully developed channel flow compared with other models (including Jonse and Launder's model[1]) and direct numerical simulation data.[7] The open symbols represent direct numerical simulation, and the lines represent the model prediction.

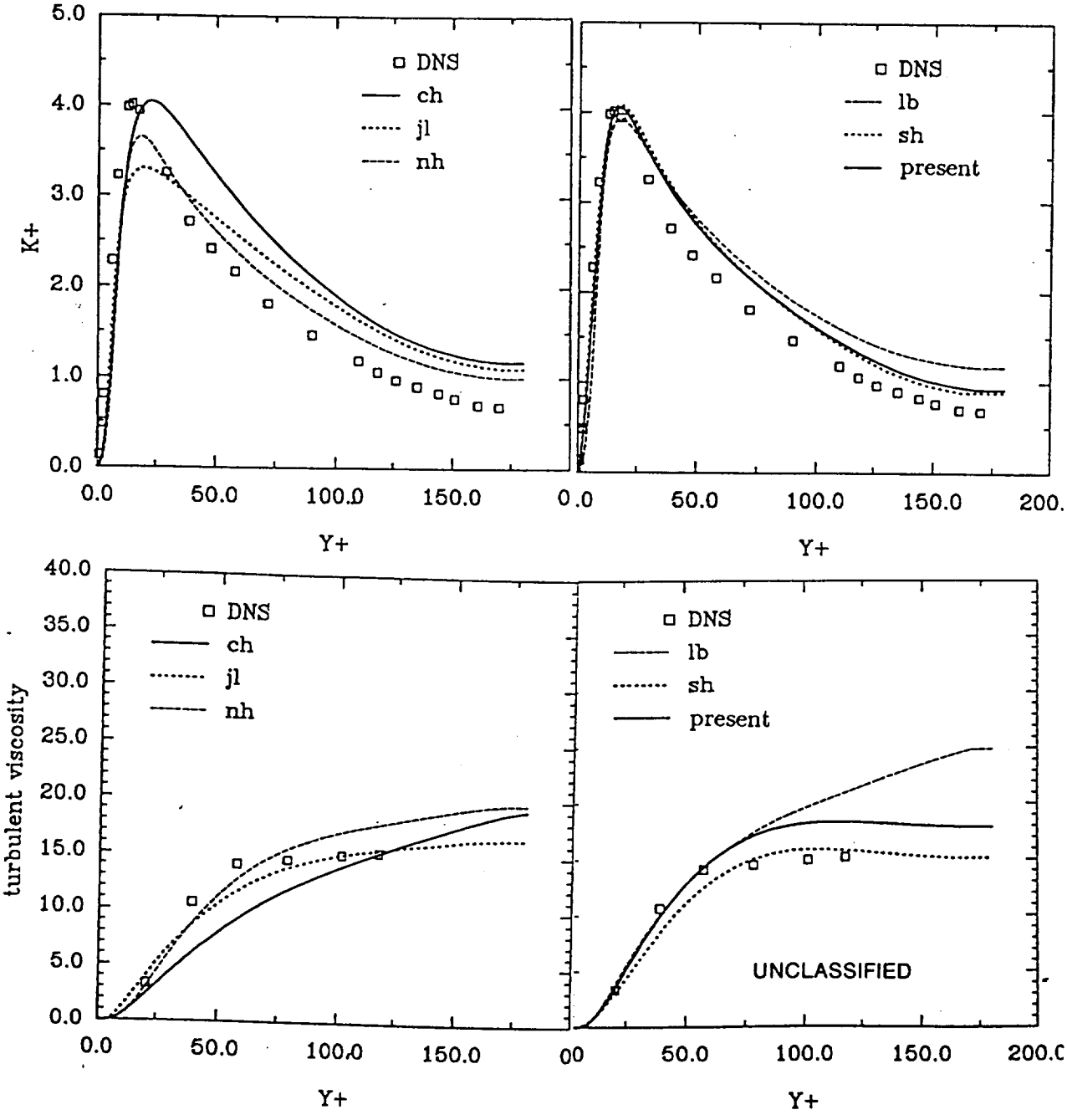

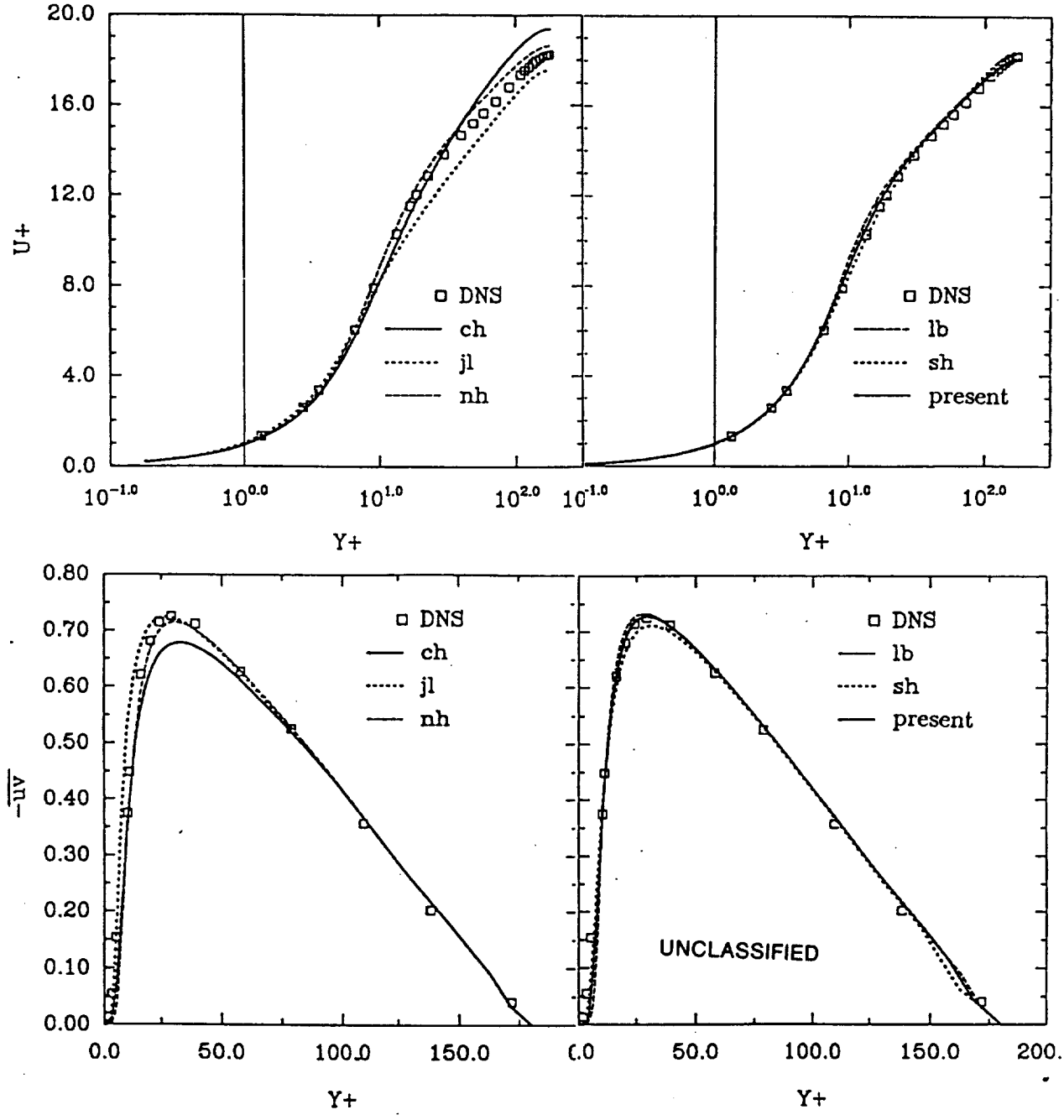
20.0
16.0
12.0
8.0
4.0
0.0
U+
DNS
ch
jl
nh
$10^{-1.0}$
$10^{0.0}$
$10^{1.0}$
$10^{2.0}$
Y+
DNS
lb
sh
present
Y+
0.80
0.70
0.60
0.50
0.40
0.30
0.20
0.10
0.00
$-\overline{uv}$
DNS
ch
jl
nh
0.0
50.0
100.0
150.0
Y+
DNS
lb
sh
present
UNCLASSIFIED
0.0
50.0
100.0
150.0
200.
Y+

2. Second order modeling of near-wall turbulence

Using the near-wall asymptotic behavior of turbulence[10] as model constraints, we formed a set of modeled transport equations for the Reynolds-stress tensor and the dissipation rate of turbulent kinetic energy. The main emphasis was on developing a near-wall model for the pressure correlation and dissipation terms in the Reynolds-stress equation. A modeled dissipation rate equation is derived more rationally. Asymptotic analysis shows that near the wall, the viscous diffusion term in the Reynolds-stress equations becomes the leading term and is balanced by the pressure correlation and dissipation terms. We use this as a model constraint in the model development. The proposed models satisfy realizibility and ensure no unphysical behavior will occur. Here, we briefly describe and list the proposed models.

Reynolds stress equation

The exact equation for the Reynolds stress tensor is:

$$\frac{D}{Dt}\langle u_i u_j\rangle = P_{ij} + T_{ij} + D_{ij}^{(\nu)} + \Pi_{ij} - \varepsilon_{ij}$$

where $\langle\ \rangle$ stands for an ensemble average, $D/Dt = \partial/\partial t + U_k \partial/\partial x_k$. the terms P_{ij}, T_{ij}, $D_{ij}^{(\nu)}$, Π_{ij} and ε_{ij} represent the production, turbulent diffusion, viscous diffusion, velocity pressure-gradient correlation and dissipation tensor, and are identified as follows:

$$\begin{aligned}
P_{ij} &= -\langle u_i u_k\rangle U_{j,k} - \langle u_j u_k\rangle U_{i,k} \\
T_{ij} &= -\langle u_i u_j u_k\rangle_{,k} \\
D_{ij}^{(\nu)} &= \nu\langle u_i u_j\rangle_{,kk} \\
\Pi_{ij} &= -\frac{1}{\rho}\langle u_i p_{,j} + u_j p_{,i}\rangle \\
\varepsilon_{ij} &= 2\nu\langle u_{i,k} u_{j,k}\rangle
\end{aligned}$$

The proposed near-wall model for $\Pi_{ij} - \varepsilon_{ij}$ is:

$$\Pi_{ij} - \varepsilon_{ij} = -f_w \frac{\epsilon}{\langle q^2\rangle}[2\langle u_i u_j\rangle + 4(\langle u_i u_k\rangle n_j n_k + \langle u_j u_k\rangle n_i n_k) + 2\langle u_k u_l\rangle n_k n_l n_i n_j]$$

where n_i is a unit vector normal to the surface, and $f_w = \exp(-(R_t/C_1)^2)$, $R_t = \frac{\langle q^2\rangle^2}{9\nu\epsilon}$, $C_1 = 1.358 R_{e\tau}^{0.44}$, $R_{e\tau} = u_\tau \delta/\nu$. u_τ is the friction velocity, δ is the thickness of the boundary layer or the half width of the channel.

Away from the wall, the velocity pressure-gradient correlation Π_{ij} is split into the rapid part $\Pi_{ij}^{(1)}$ and the slow part $\Pi_{ij}^{(2)}$:

$$\Pi_{ij} = \Pi_{ij}^{(1)} + \Pi_{ij}^{(2)}$$

The proposed model for $\Pi_{ij}^{(2)} - \varepsilon_{ij}$ is:

$$\Pi_{ij}^{(2)} - \varepsilon_{ij} = -\epsilon(\beta b_{ij} + \frac{2}{3}\delta_{ij})(1 - f_w)$$

where

$$\beta = 2 + \frac{F}{9}\{\frac{72}{R_t^{1/2}} + 80.1\ln[1 + 62.4(-II + 2.3III)]\}\exp(-\frac{7.77}{R_t^{1/2}})$$

$$F = 1 + 27III + 9II$$

$$II = -\frac{1}{2}b_{ij}b_{ji}$$

$$III = \frac{1}{3}b_{ij}b_{jk}b_{ki}$$

$$b_{ij} = \langle u_i u_j\rangle/\langle q^2\rangle - \delta_{ij}/3$$

The rapid part of velocity pressure-gradient, $\Pi_{ij}^{(1)}$ is modeled as follows(Shih and Lumley[11,12]):

$$\begin{aligned}\Pi_{ij}^{(1)} &= (\frac{1}{5} + 2a_5)\langle q^2\rangle(U_{i,j} + U_{j,i}) - \frac{2}{3}(1 - a_5)(P_{ij} - \frac{2}{3}P\delta_{ij}) \\ &+ (\frac{2}{3} + \frac{16}{3}a_5)(D_{ij} - \frac{2}{3}P\delta_{ij}) + \frac{2}{15}(P_{ij} - D_{ij}) + \frac{6}{5}b_{ij}P \\ &+ \frac{2}{5\langle q^2\rangle}[(\langle u_i u_k\rangle U_{j,q} + \langle u_j u_k\rangle U_{i,q})\langle u_k u_q\rangle - \langle u_i u_p\rangle\langle u_j u_q\rangle(U_{p,q} + U_{q,p})]\end{aligned}$$

where,

$$P_{ij} = -\langle u_i u_k\rangle U_{j,k} - \langle u_j u_k\rangle U_{i,k}$$

$$D_{ij} = -\langle u_i u_k\rangle U_{k,j} - \langle u_j u_k\rangle U_{k,i}$$

$$P = \frac{1}{2}P_{ii}$$

$$a_5 = -\frac{1}{10}(1 + C_2 F^{1/2})$$

$$C_2 = 0.8[1 - \exp(-(R_t/40)^2)]$$

Finally the model for the third moments is modeled as:

$$\langle u_i u_j u_k\rangle = -.07\frac{\langle q^2\rangle}{2\epsilon}[\langle u_k u_p\rangle\langle u_i u_j\rangle_{,p} + \langle u_j u_p\rangle\langle u_i u_k\rangle_{,p} + \langle u_i u_p\rangle\langle u_j u_k\rangle_{,p}]$$

Dissipation rate equation

The modeled dissipation rate equation derived in this work is:

$$\begin{aligned}\epsilon_{,t} + U_i\epsilon_{,i} &= (\nu\epsilon_{,i} - \langle\epsilon u_i\rangle)_{,i} - \psi_0\frac{\epsilon\tilde{\epsilon}}{\langle q^2\rangle} \\ &- \psi_1\frac{\tilde{\epsilon}}{\langle q^2\rangle}\langle u_i u_j\rangle U_{i,j} - \psi_2\frac{\nu\langle q^2\rangle}{\epsilon}\langle u_k u_l\rangle(U_{i,jl} - U_{l,ij})U_{i,jk}\end{aligned}$$

where

$$\psi_0 = \frac{14}{5} + 0.98[1 - 0.33\ln(1 - 55II)]\exp(-2.83R_t^{-1/2})$$

$$\psi_1 \approx 2.1$$

$$\psi_2 = -.15(1 - F)$$

$$\tilde{\epsilon} = \epsilon - \frac{\nu\langle q^2\rangle_{,i}\langle q^2\rangle_{,i}}{4\langle q^2\rangle}$$

The turbulent flux term $\langle \epsilon u_k \rangle$ is modeled as:

$$\langle \epsilon u_k \rangle = -.07\frac{\langle q^2\rangle}{2\epsilon}\langle u_k u_p\rangle \epsilon_{,p}$$

These figures show some existing Reynolds stress models (for example, Launder and Shima[13], Lai and So[14]) and present model compared with the direct numerical simulations.[7]

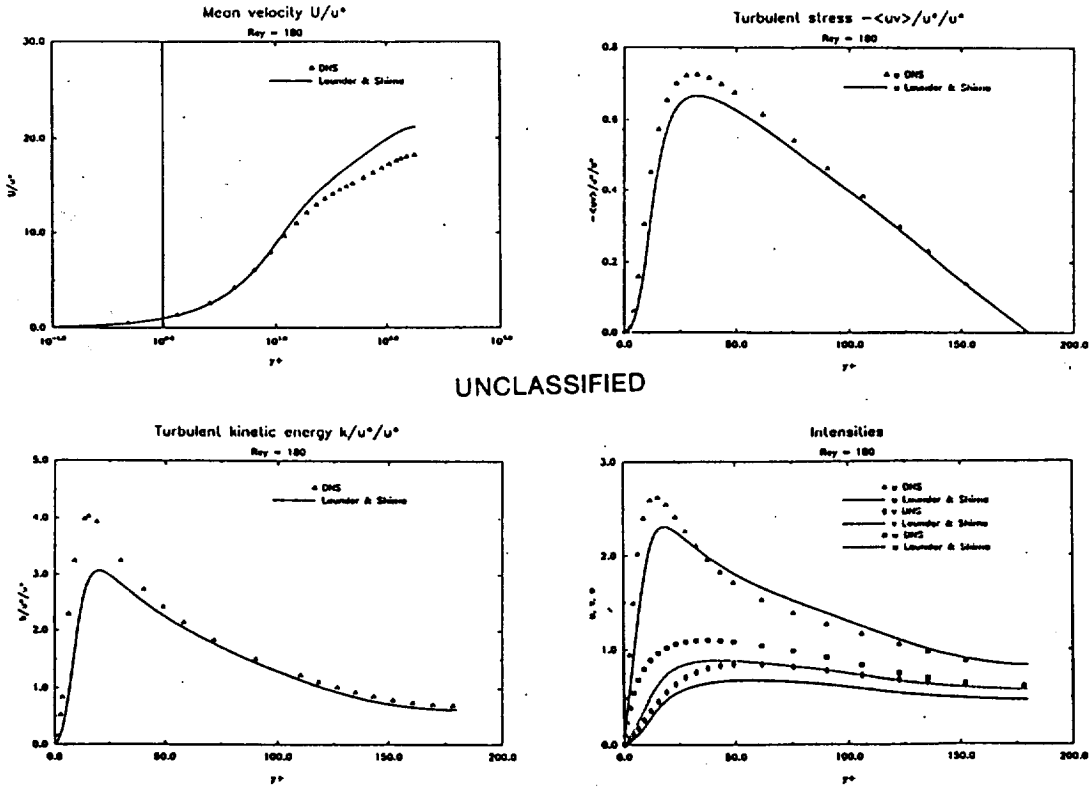

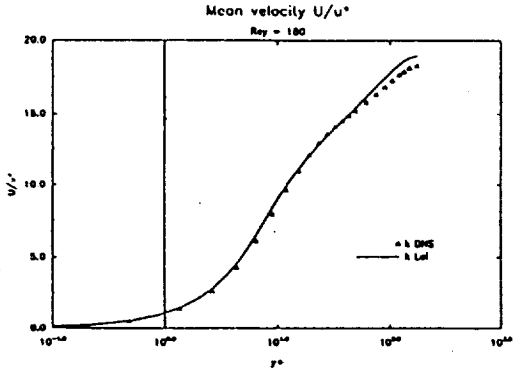

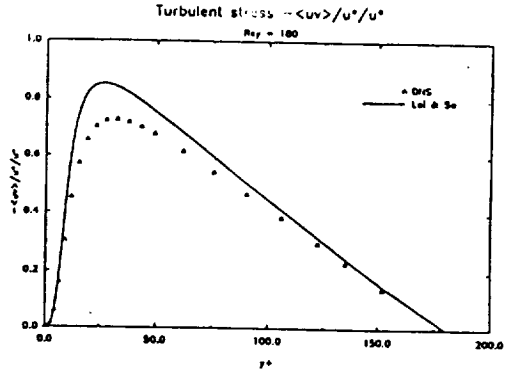

UNCLASSIFIED

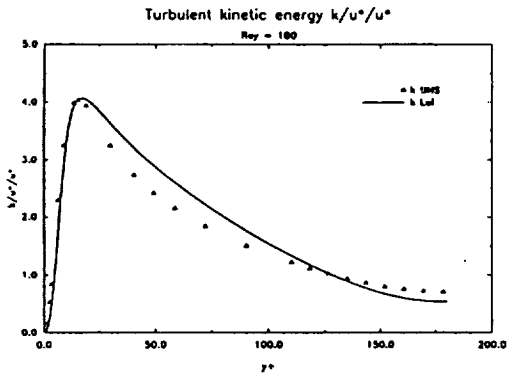

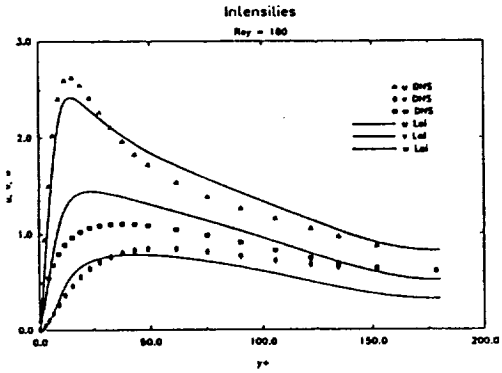

U – MEAN VELOCITY

K – KINETIC ENERGY

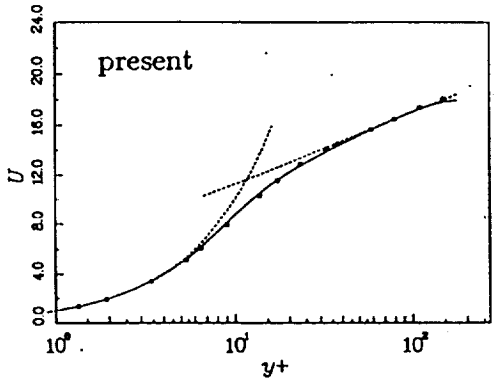

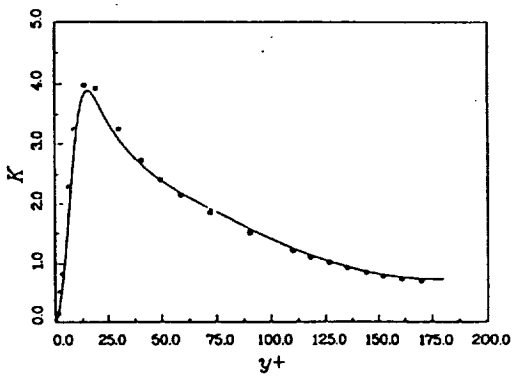

u, v, w — RMS OF FLUCTUATING VELOCITY

<UV> PROFILE

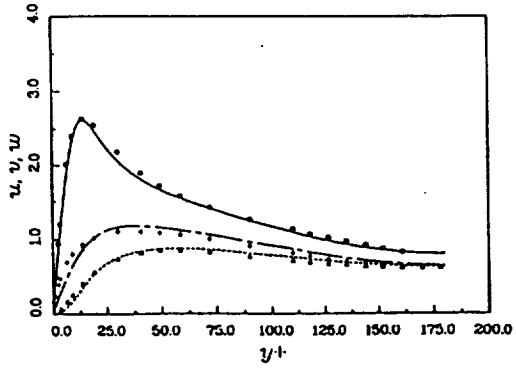

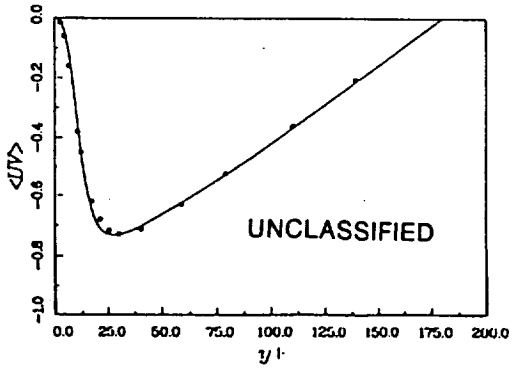

3. Second order modeling of a three-dimensional boundary layer

A study[15] of three-dimensional effects on turbulent boundary layer were achieved by direct numerical simulation of a fully developed turbulent channel flow subjected to transverse pressure gradient. The results show that, in agreement with experimental data[16], the Reynolds stresses are reduced with increasing three-dimensionality and that, near the wall, a lag develops between the stress and the strain rate. To model these three-dimensional effects on the turbulence, we have tried various two equation models and second order closure models. None of the current models can predict the reductions in the shear stress observed using direct numerical simulations. However, we found that the newly proposed second order closure model listed in the previous section do at least qualitatively capture these three-dimensional effects.

The following figures show the direct numerical simulation of the three dimensional boundary layer flow and the model predictions from Launder and Shima, Lai and So and the present models.

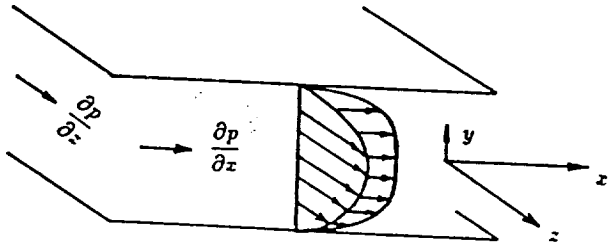

Schematic of three-dimensional channel flow.

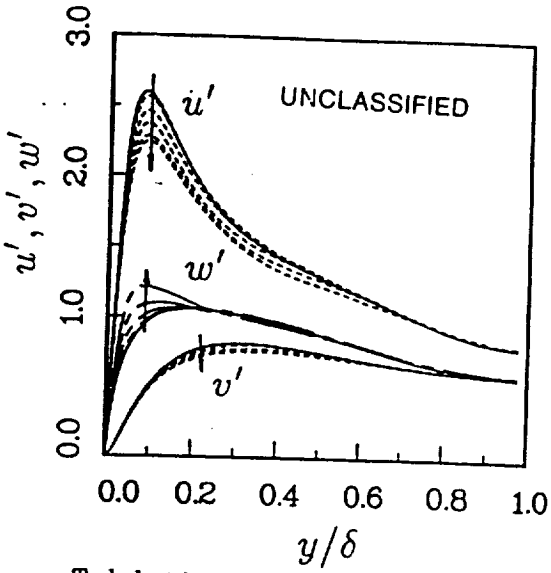

Turbulent intensities in fixed coordinates at Δt = 0.15 intervals.

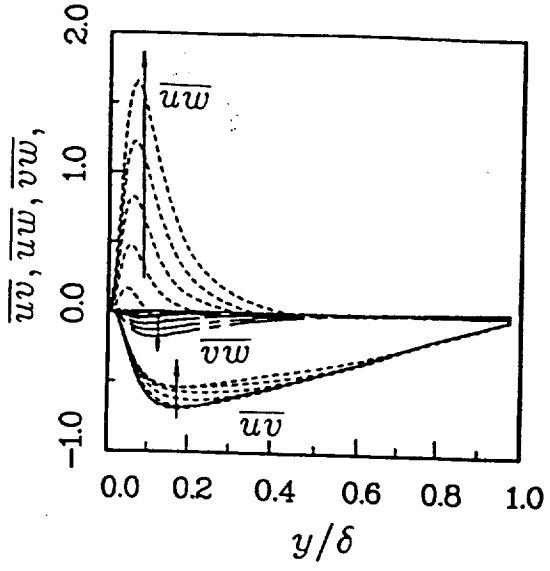

Reynolds stress component in fixed coordinate at Δt = 0.15 intervals.

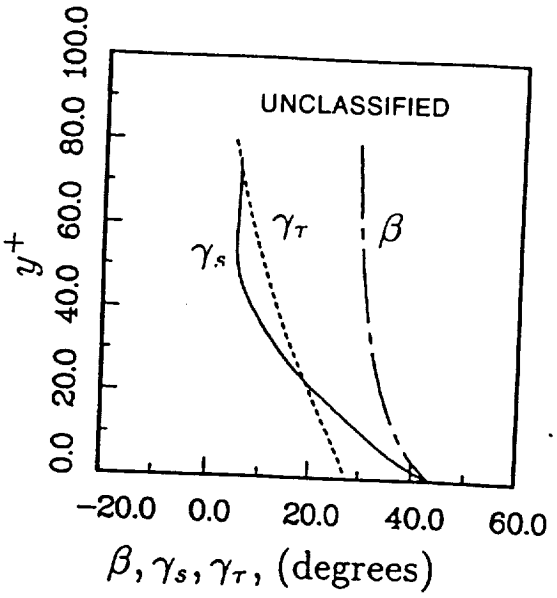

Distribution across the channel of the mean flow angle (———), the Reynolds shear stress angle (- - - -), and the mean velocity gradient angle (———).

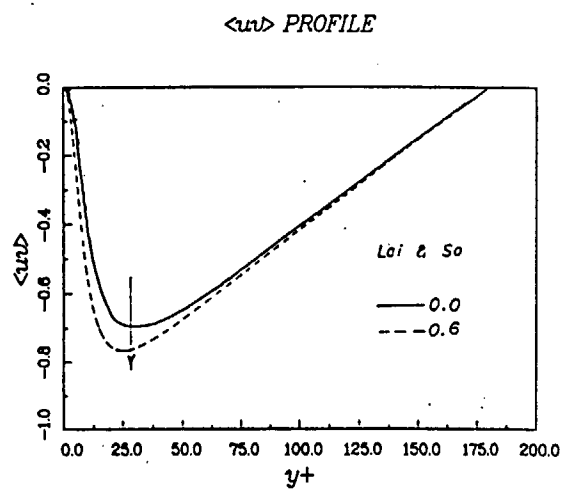
<uv> PROFILE
Lai & So
0.0
0.6
<uv>
y+

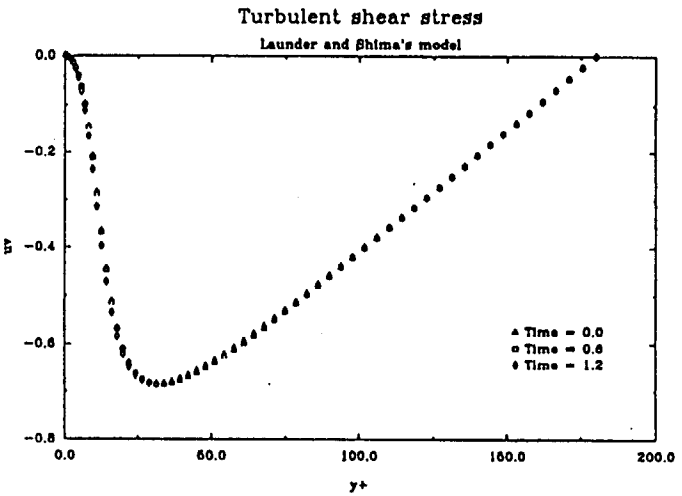
Turbulent shear stress
Launder and Shima's model
Time = 0.0
Time = 0.6
Time = 1.2
y+

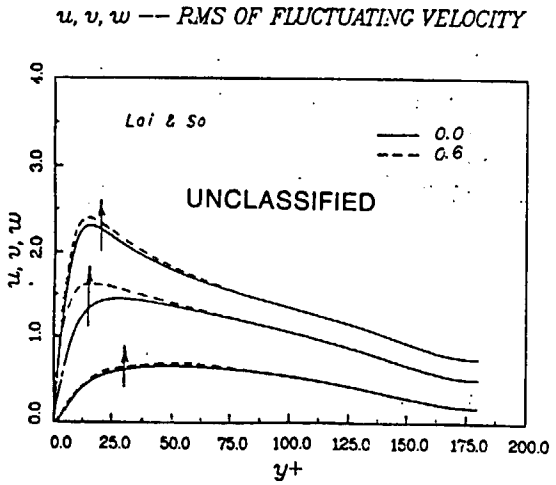
u, v, w -- RMS OF FLUCTUATING VELOCITY
Lai & So
0.0
0.6
UNCLASSIFIED
u, v, w
y+

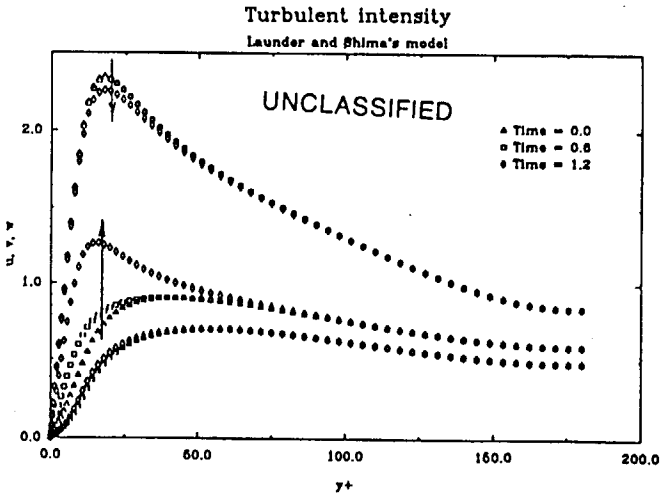
Turbulent intensity
Launder and Shima's model
UNCLASSIFIED
Time = 0.0
Time = 0.6
Time = 1.2
y+

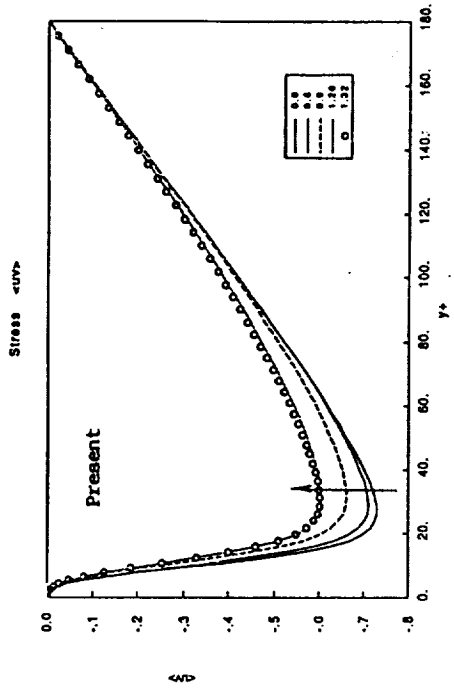
Present
Stress <uv>
y+

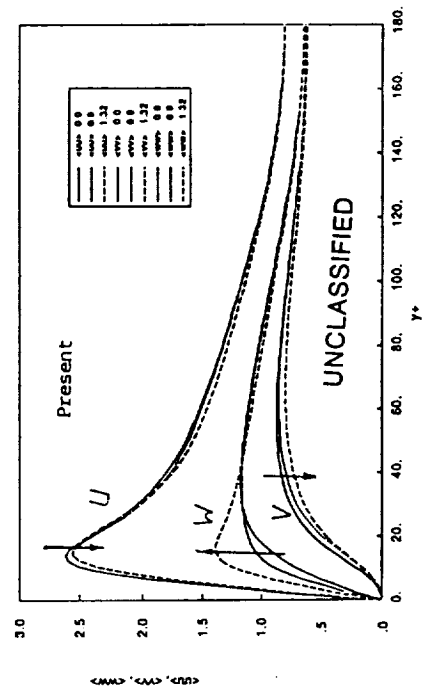
Present
U
W
V
UNCLASSIFIED
RMS of fluctuating velocities
y+

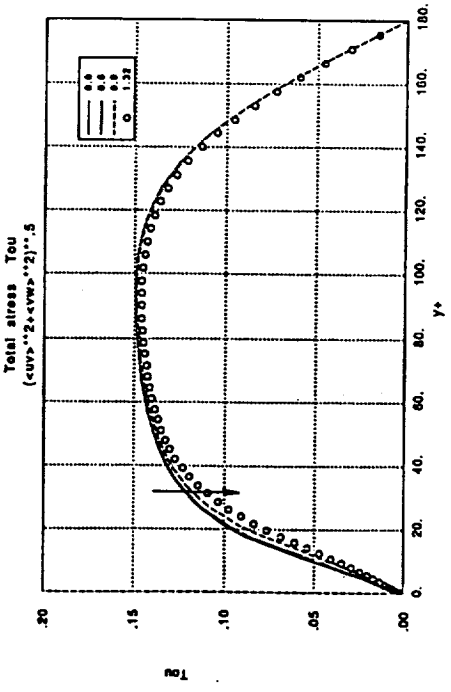
Total stress Tou
(<uv>**2+<vw>**2)**.5
y+

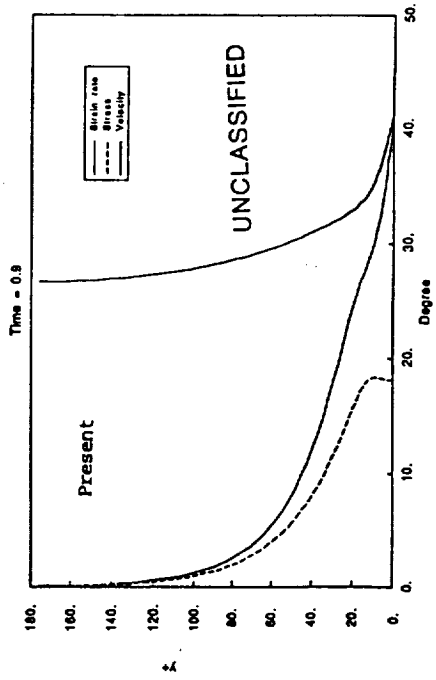
Present
UNCLASSIFIED
Time = 0.8
Degree
y+

References

1. Jones, W.P. and Launder, B.E., "The Calculation of Low-Reynolds Number Phenomena with a Two-Equation model of Turbulence," *International Journal of Heat and Mass Transfer*, Vol. 16, 1973, pp. 1119-1130.
2. Lam, C.K.G. and Bremhorst, K., "A Modified Form of the $K-\epsilon$ Model for Predicting Wall Turbulence," *ASME Transactions, Journal of Fluids Engineering*, Vol. 103, Sept. 1981, pp.456-460.
3. Chien, K.-Y., "Predictions of Channel and Boundary-Layer Flow with a Low-Reynolds-Number Turbulence Model," *AIAA Journal*, Vol. 20, Jan. 1982, pp. 33-38.
4. Nagano, Y. and Hishida, M., "Improved Form of the $K-\epsilon$ Model for Wall Turbulent Shear Flows," *ASME Transaction, Journal of Fluids Engineering*, Vol. 109, June 1987.
5. C.G. Speziale, R. Abid and E. Clay Anderson, "A Critical Evaluation of Two-Equation Models for Near Wall Turbulence," AIAA 21st Fluid Dynamics, Plasma Dynamics and Laser Conference, June 18-20, 1990/Seattle, WA.
6. T.-H. Shih, " An Improved k-ϵ Model for Near-Wall Turbulence and Comparison with Direct Numerical Simulation," NASA TM 103221, ICOMP-90-16.
7. Kim, J., Moin, P. and Moser, Robert., "Turbulent statistics in fully developed channel flow at low Reynolds number," *J. Fluid Mech.*, 177, 1987, pp. 133–166.
8. P.R. Spalart,"Direct simulation of a turbulent boundary layer up to $R_\theta = 1410$," bf J. Fluid Mech., vol. 187, 1988, pp. 61-98.
9. V. Michelassi, personal communication, 1990.
10. Mansour, N.N., Kim,J. and Moin. P., "Reynolds–Stress and Dissipation Rate Budgets in a Turbulent Channel Flow," *J. Fluid Mech.*, Vol. 194, 1988, pp. 15–44.
11. Shih, T.H. and Lumley, J.L., " Modeling of pressure correlation terms in Reynolds–stress and scalar flux equations," Rept. FDA-85-3, Sibley School of Mech. and Aerospace Eng., Cornell University.
12. Shih, T.H. and Lumley J.L., " Second-order modeling of near-wall turbulence," *Phys. Fluids*, 29, 1986, pp. 971–975.
13. Launder, B.E. and Shima, N., "Second-Moment Closure for the Near-Wall Sublayer: Development and Application," *AIAA Journal*, Vol. 27, Oct. 1989, pp. 1319-1325.
14. Lai, Y.G. and So, R.M.C., *Int. J. Heat Mass Transfer*, to appear(1990).
15. Moin, P., Shih, T.H., Driver, D. and Mansour, N.N., "Numerical Simulation of a Three-Dimensional Turbulent Boundary Layer," AIAA 89-0373.
16. Bradshaw, P. and Pontikos, N., "Measurements in the Turbulent Boundary Layer on an Infinite Swept-Wing," **J. Fluid Mech**, 159, 1985, pp. 105-130.

SOURCE: NASA TM 104369, ICOMP-91-07, CMOTT-91-02

Second Order Modeling of Boundary–Free Turbulent Shear Flows

T.-H. Shih
Institute for Computational Mechanics in Propulsion
and Center for Modeling of Turbulence and Transition
Lewis Research Center
Cleveland, Ohio

J.-Y. Chen
Sandia National Laboratories
Livermore, California

J.L. Lumley
Cornell University
Ithaca, New York

Abstract

This paper presents a set of realizable second order models for boundary free turbulent flows. The constraints on second order models based on the realizability principle are re-examined. The rapid terms in the pressure correlations for both the Reynolds stress and the passive scalar flux equations are constructed to exactly satisfy the joint realizability. All other model terms (return-to-isotropy, third moments and terms in the dissipation equations) already satisfy realizability (Lumley 1978, Shih and Lumley 1986). To correct the spreading rate of the axisymmetric jet, an extra term is added to the dissipation equation which accounts for the effect of mean vortex stretching on dissipation. The test flows used in this study are the mixing shear layer, plane jet, axisymmetric jet and plane wake. The numerical solutions show that the new unified model equations (with unchanged model constants) predict all these flows reasonably as the results compare well with the measurements. We expect that these model equations would be suitable for more complex and critical flows.

A. Shabbir
Visiting Assistant Professor.

D. B. Taulbee
Professor.
Mem. ASME

Department of Mechanical and Aerospace Engineering,
University at Buffalo, SUNY
Amherst, NY 14260

Evaluation of Turbulence Models for Predicting Buoyant Flows

Experimental data for the buoyant axisymmetric plume are used to validate certain closure hypotheses employed in turbulence model equations for calculating buoyant flows. Closure formulations for the turbulent transport of momentum, thermal energy, kinetic energy, and squared temperature used in the k–ε and algebraic stress models are investigated. Experimental data for the mean velocity, mean temperature, and kinetic energy are used in the closure formulation to obtain Reynolds stresses, heat fluxes, etc., which are then compared with their measured values.

1 Introduction

Various turbulence models have been formulated for predicting buoyancy-driven flows. Some of the parameters in these models have been determined by keying the solution of the model equations to experimental data for certain basic flows such as decay of grid turbulence. Other parameters have been determined by calibrating closure formulations directly with experimental data. However, this approach may be somewhat inaccurate due to the lack of quality experimental data for certain correlations, especially dissipation. Finally, certain model parameters have been fine tuned or determined by requiring that the computed solution agree with experimental data for more complex flows, such as shear flows. In addition there have been instances where model parameters have been adjusted or empirical corrective terms added so that agreement with experimental data is accomplished for a particular flow. When model parameters are adjusted to get agreement, say for the mean velocity and temperature fields for a particular flow, little regard is given for the internal integrity of the model. In other words, are the various processes such as diffusional transport, pressure-strain interactions, etc., predicted correctly? Or are there compensating assumptions where one process is overpredicted at the expense of another and yet the end predicted result for the mean flow agrees with experiment? The lack of complete sets of data for higher moments, dissipation, and pressure–velocity correlations for various flows has prevented detailed verification of closure models for the various processes that have to be modeled.

The objective of this paper is to use the recently obtained and comprehensive experimental data of Shabbir and George (1987) and Shabbir (1987) on the axisymmetric buoyant plume to assess the various closure relations proposed for the kinetic-energy/dissipation and the algebraic stress models for buoyancy-dominated flows. The usual approach is to solve the modeled differential equations numerically, and then compare the computations with the experiment. However, this method does not help pinpoint the drawbacks in the various terms of the models. In this paper, instead of the usual approach, correlations obtained from measured velocity and temperature are used directly to verify the closure hypotheses for the turbulent transport of momentum, thermal energy, and turbulent kinetic energy.

2 Experimental Data

The data used were taken in an axisymmetric buoyant plume by Shabbir and George (1987) and Shabbir (1987), who measured velocity and temperature fields at several vertical levels above a heated source of air. Here we briefly summarize their experimental technique and results.

The three-wire probe used consisted of a cross-wire and a temperature wire. Thus the instantaneous values of the two velocity components (vertical and radial) and temperature were measured. The axisymmetry of the flow was established by using an array of 16 thermocouples and also by rotating the cross-wire by 90 deg. Profiles for the correlations between the velocity components and velocity components with temperature through the fourth order were determined from the instantaneous measurements.

Source conditions were continuously monitored in order to calculate the rate at which buoyancy was added at the source. The source Grashof number was 5.5. By integrating the mean energy equation, an integral constraint can be obtained for a buoyant plume. For a neutral environment this constraint implies that the rate at which buoyancy crosses each horizontal section is constant and must equal the rate at which buoyancy is added at the source, i.e., the ratio

$$\frac{F}{F_o} = \frac{1}{F_o}\left[2\pi \int_0^\infty g\beta(U\Delta T + \overline{ut})r\,dr\right] \tag{1}$$

must be unity (F_o is the source buoyancy). This integral constraint was satisfied within 7 percent.

The correlation profiles at various heights were found to be similar in the coordinate $\eta = r/z$ (z accounted for the virtual origin) when the velocity is scaled by $U_s F_o^{1/3} z^{-1/3}$ and the temperature is scaled by $T_s = F_0^{2/3} z^{-5/3}/g\beta$. The measurements agreed well with the earlier study by George et al. (1977), who measured only the temperature and the vertical component of velocity. The scatter in the measurements of higher moments is typical for such flows and is also present in previous experiments, such as those of George et al. (1977). The primary reason for the scatter is that slow time scales of the flow require much longer averaging time for the higher moments in order to obtain the same statistical convergence as for the mean quantities. Other errors in the measurements arise from the flow reversal on the hot wire—a phenomenon most likely to occur toward the outer edges of the flow where local turbulent intensities are considerably higher. These are discussed in Shabbir and George (1987).

The various correlations in similarity variables were fitted with curves using a least-squares fitting procedure. This representation allows easy evaluation of the terms in the governing equations and closure formulations when they are cast in similarity variables. Using these profiles the balances for the mean momentum and energy differential equations were carried out to check whether the flow satisfied the equations of motion it is supposed to represent. Within the thin shear layer and the Boussinesq assumption the mean momentum and energy equa-

Contributed by the Heat Transfer Division and presented at the National Heat Transfer Conference, Pittsburgh, Pennsylvania, August 9–12, 1987. Manuscript received by the Heat Transfer Division March 3, 1988; revision received November 10, 1989. Keywords: Modeling and Scaling, Plumes, Turbulence.

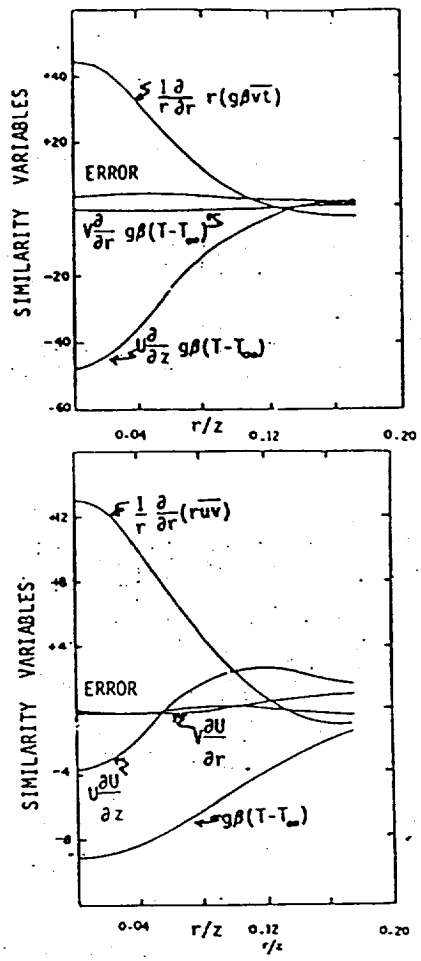

Fig. 1(*a*) Balances of mean energy and momentum equations (taken from Shabbir and George, 1987)

tions can be respectively written as

$$U\frac{\partial U}{\partial z} + V\frac{\partial U}{\partial r} = -\frac{1}{r}\frac{\partial}{\partial r}(r\overline{uv}) - g\beta\Delta T \tag{2}$$

$$U\frac{\partial \Delta T}{\partial z} + V\frac{\partial \Delta T}{\partial r} = -\frac{1}{r}\frac{\partial}{\partial r}(r\overline{vt}) \tag{3}$$

Since all the quantities appearing in these equations are measured, their profiles were substituted to see whether the measurements balance the equations. Figure 1(*a*), taken from Shabbir and George (1987), shows that the experiment satisfies this nontrivial test within 10 percent. An error of such magnitude is typical of turbulent shear flows.

The dissipation of mechanical energy was determined by balancing the turbulent energy equation

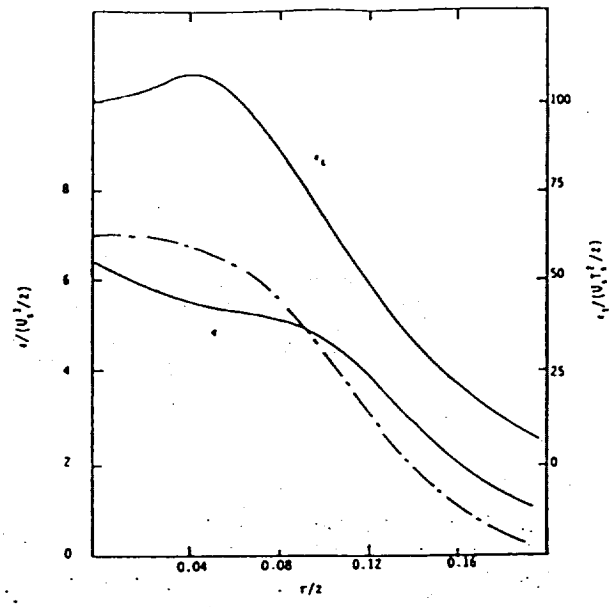

Fig. 1(*b*) Mechanical and thermal dissipation profiles! Full lines are experimental; the chained line is from model equation (10), which was solved for ϵ with all other quantities taken from experiment.

$$U_j\frac{\partial k}{\partial x_j} = -\frac{\partial}{\partial x_j}\left(\frac{1}{2}\overline{q^2u_j} + \frac{1}{\rho}\overline{pu_j}\right) + P + G - \epsilon \tag{4}$$

where $P = -\overline{u_iu_j}\,\partial U_i/\partial x_j$ is the mechanical production and $G = -\beta g_i\overline{u_it}$ is the production due to buoyancy. Each term except for the dissipation ϵ and the pressure transport $\overline{pu_i}$ is determined from the experimentally determined correlations. The pressure transport was evaluated from $\overline{pu_j}/\rho = -q^2u_j/5$, a formula given by Lumley (1978). Although this closure relation has not been verified experimentally, it was felt that since the pressure transport is significant, some correction should be included rather than simply neglecting it, as is often done. The dissipation determined from the balance of the turbulent kinetic energy equation is shown in Fig. 1(*a*) as a solid line.

By a similar procedure the dissipation of the mean-square temperature t^2 is determined from

$$U_j\frac{\partial \overline{t^2}}{\partial x_j} = -\frac{\partial}{\partial x_j}\overline{u_jt^2} - 2\,\overline{u_jt}\frac{\partial T}{\partial x_j} - 2\epsilon_t \tag{5}$$

All terms are evaluated from experimental data and the resulting thermal dissipation is shown in Fig. 1(*b*).

The time scales $\overline{q^2}/\epsilon$ and $\overline{t^2}/\epsilon_t$ for the relaxation of the mechanical and thermal dissipation, respectively, are shown in Fig. 2, along with their ratio

$$R = (\overline{t^2}/\epsilon_t)/(\overline{q^2}/\epsilon) \tag{6}$$

Nomenclature

F_o = buoyancy flux, equation (1)
g = acceleration due to gravity
G = turbulence production from buoyancy
k = turbulent kinetic energy
p = fluctuating pressure
P = turbulence production by mean flow
Pr_T = turbulent Prandtl number
r = radial coordinate
R = time scale ratio, equation (4)
t = fluctuating temperature
T = mean temperature
u = fluctuating axial velocity component
U = mean axial velocity component
v = fluctuating radial velocity component
z = vertical coordinate
β = coefficient of thermal expansion
ϵ = dissipation of mechanical energy
ϵ_t = dissipation of mean-square temperature
ν_T = turbulent eddy viscosity
ρ = mean density

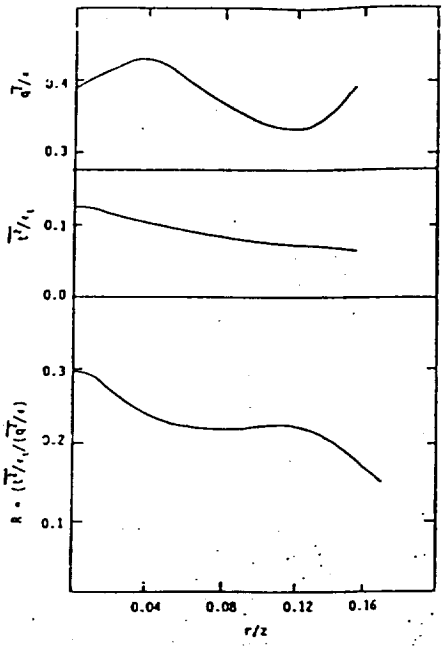

Fig. 2 Mechanical and thermal time scale ratios and variation of R as calculated from experimental data

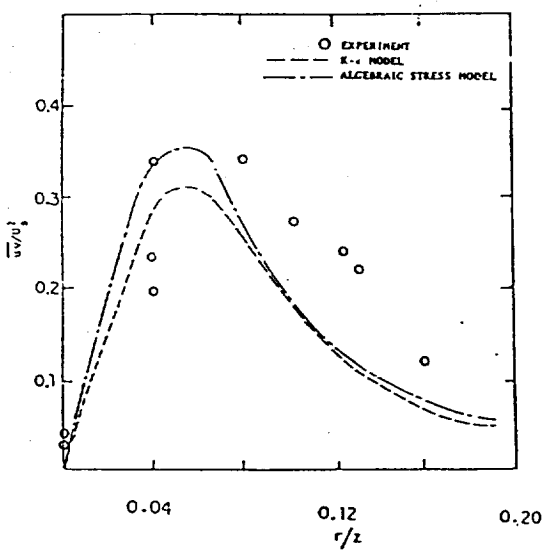

Fig. 3 Shear stress

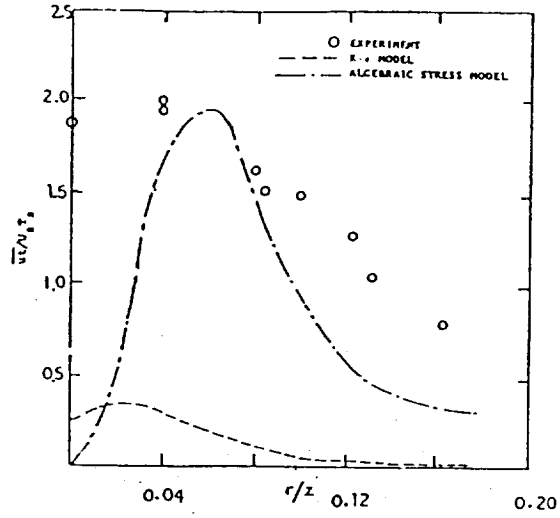

Fig. 4 Axial heat flux

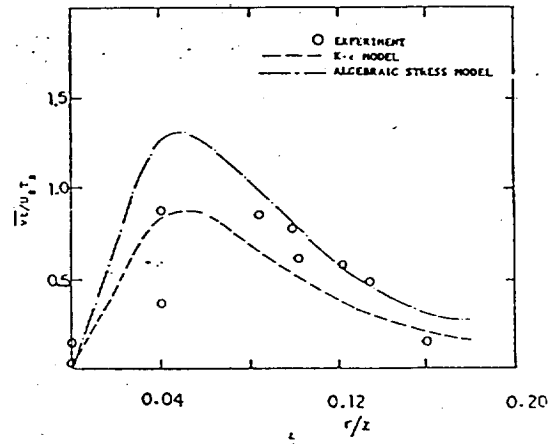

Fig. 5 Radial heat flux

These time scales appear extensively throughout the model formulations and will be further discussed in the next sections.

3 Assessment of Closure Hypotheses of k–ε Model

The form of the k–ϵ model, which is considered to be the standard one, is that used by Launder and Spalding (1974). In this model the Reynolds stress is given by

$$-\overline{u_i u_j} = \nu_T \left(\frac{\partial U_i}{\partial x_j} + \frac{\partial U_j}{\partial x_i} \right) - \frac{2}{3} k \delta_{ij} \tag{7}$$

and the heat flux by

$$-\overline{u_i t} = \frac{\nu_T}{\mathrm{Pr}_T} \frac{\partial T}{\partial x_i} \tag{8}$$

where $\nu_T = C_\mu k^2/\epsilon$ and $C_\mu = 0.09$ (see Launder and Spalding, 1974).

By invoking the thin shear layer assumption for a buoyant plume, the above relations reduce to

$$\overline{uv} = -\nu_T \frac{\partial U}{\partial r}$$

$$\overline{ut} = -(\nu_T/\mathrm{Pr}_T) \frac{\partial T}{\partial z}$$

$$\overline{vt} = -(\nu_T/\mathrm{Pr}_T) \frac{\partial T}{\partial r}$$

Taking $\mathrm{Pr}_T = 1.0$, the right-hand sides of the above equations were evaluated experimentally. These are compared with measured values of $\overline{uv}$, $\overline{ut}$, and $\overline{vt}$ in Figs. 3–5. The points are experimental values and the chain lines are from the model.

The modeled values of $\overline{uv}$ and $\overline{vt}$ compare reasonably with the experimental profiles except in the outer portion of the curves. On the other hand the modeled profile of vertical heat flux $\overline{ut}$ is much smaller than the experimental one. It is well known that the simple gradient models given by equations (7) and (8) with an isotropic eddy viscosity are inadequate for determining streamwise turbulent momentum and heat fluxes. Usually these quantities do not influence the prediction for shear layers since only the radial fluxes are important in these flows. However, in the case of the buoyant plume the flux $\overline{ut}$ is a dominant production term in the turbulent kinetic energy

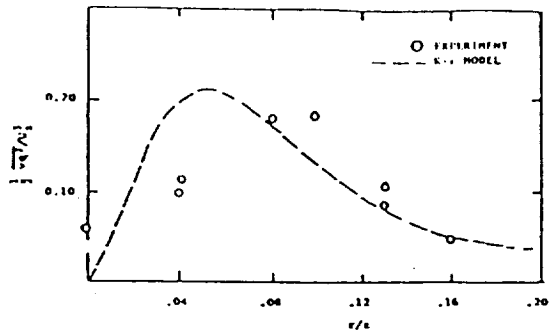

Fig. 6 Transport of kinetic energy

equation and its correct calculation is very important for accurate prediction of k.

The diffusional transport in the kinetic energy equation (4) for a thin shear layer is modeled as

$$\frac{1}{2}\overline{vq^2} + \frac{1}{\rho}\overline{pv} = -\nu_T \frac{\partial k}{\partial r} \tag{9}$$

Using $\overline{pv}/\rho = -\overline{vq^2}/5$ from Lumley (1978) gives $\overline{vq^2}/2 = -(5/3)\nu_T \partial k/\partial r$ from which the result, with the right side evaluated from experimental results, is shown in Fig. 6. It is seen that the predicted and experimental data peak at different radial locations; however, the predicted magnitude is more accurate, which indicates that the pressure diffusion needed to be taken into account.

In the k-ϵ model the dissipation is calculated from

$$U_j \frac{\partial \epsilon}{\partial x_j} = -\frac{\partial}{\partial x_j}\overline{\epsilon' u_j} + C_{\epsilon 1}\frac{\epsilon}{k}(P+G) - C_{\epsilon 2}\frac{\epsilon^2}{k} \tag{10}$$

where $\overline{\epsilon' u_j} = -(\nu_T/\sigma_\epsilon)\partial\epsilon/\partial x_j$ and $\sigma_\epsilon = 1.3$, $C_{\epsilon 1} = 1.44$, and $C_{\epsilon 3} = 1.92$ as given by Launder and Spalding (1974). In order to get an indication of the validity of equation (10), it was numerically solved for the dissipation ϵ with all other quantities needed to evaluate the coefficients determined from the experimental correlations. The result is shown in Fig. 1(b) and it is seen that it compares reasonably well with the curve obtained from balancing the turbulent kinetic energy equation with experimental data.

Launder et al. (1972) showed that the standard k-ϵ model yields a solution for the axisymmetric jet that overpredicts the spreading rate by about 30 percent. The standard k-ϵ model also does not correctly predict the axisymmetric buoyant plume (Hossain and Rodi, 1982). Proposals have been made (Pope, 1978; Hanjalic and Launder, 1980) for modifying the dissipation equation, based on arguments concerned with vortex or eddy structures characteristic of axisymmetric flows. The modified equation produces more dissipation, thus decreasing the turbulent eddy viscosity, which results in a smaller spreading rate of the flow. Here we use the empirical correction given by Rodi (1972) where $C_{\epsilon 2} = 1.92(1-0.035H)$ with $H = 1/(y_E/U_m)dU_m/dx|^{0.2}$ and where U_m is the maximum velocity and y_E is the distance from the centerline to the edge of the shear layer. This correction decreases the destruction term in the dissipation equation, hence producing an increased dissipation. However, when this correction is used in equation (10) there is very little change in the solution for ϵ when experimental data are used for the other quantities in the equation. This is probably due to the approach taken here, which does not allow for the nonlinear interactions between the various terms in the closure. If the kinetic energy and dissipation equations are solved simultaneously, then the axisymmetric correction will produce a significant change in the solution of the k-ϵ model.

4 Assessment of Closure Hypotheses for Algebraic Stress Model

Chen and Rodi (1975), Tamanini (1978), Chen and Chen (1979), and Hossain and Rodi (1982) have made predictions for the buoyant jet using algebraic stress models. Many of the ideas used in these models for calculating buoyant flows originated with Launder (1975, 1978). Algebraic stress models are obtained by simplifying the convective transport equations for Reynolds stresses and heat fluxes so they are no longer differential equations. The dynamic equation for the Reynolds stress tensor is

$$(C-D)\overline{u_iu_j} = P_{ij} + G_{ij} - \frac{2}{3}\epsilon\delta_{ij} - C_1\epsilon\left(\frac{\overline{u_iu_j}}{k} - \frac{1}{3}\delta_{ij}\right) - C_2\left(P_{ij} - \frac{2}{3}P\delta_{ij}\right) - \frac{30C_2-22}{5}\left(D_{ij} - \frac{2}{3}P\delta_{ij}\right) - (8C_2-6)k\left(\frac{\partial U_i}{\partial x_j} + \frac{\partial U_j}{\partial x_i}\right) - C_3\left(G_{ij} - \frac{2}{3}G\delta_{ij}\right) \tag{11}$$

where $P_{ij} = -\overline{u_iu_k}\,\partial U_j/\partial x_k - \overline{u_ju_k}\,\partial U_i/\partial x_k$ is the mechanical production and $G_{ij} = -\beta g_i\,\overline{u_j\theta} - \beta g_j\,\overline{u_i\theta}$ is the buoyancy production. The left side represents convection minus diffusional transport, the dissipation is assumed isotropic, and the last three lines represent the closure formulation for $p(\partial u_i/\partial x_j + \partial u_j/\partial x_i)/\rho$ given by Launder et al. (1975) and Launder (1975, 1978). Launder assumes: (1) an equilibrium situation where convection is balanced by diffusion ($C - D = 0$) and production is balanced by dissipation ($P + G - \epsilon = 0$); (2) the second and third terms (third line) in the rapid part of the pressure-velocity correlation are negligible; the coefficient C_2 is adjusted so that the first term approximates the entire rapid part; (3) the parameter C_3 is taken equal to C_2. After applying all the assumptions

$$\overline{u_iu_j} = \frac{2}{3}\frac{C_1+C_2-1}{C_1}k\delta_{ij} - \frac{1-C_2}{C_1}\frac{k}{\epsilon}(P_{ij}+G_{ij}) \tag{12}$$

where $c_1 = 2.2$ and $C_2 = 0.6$. It should be pointed out that in free shear flows the equilibrium condition ($C - D = 0$ and $P + G - \epsilon = 0$) only applies in the outer portion of the flow. Also, Zeman and Lumley (1976) found $C_3 = 0.3$, after applying all the constraints applicable to determining the contribution of buoyancy to the pressure-strain correlation.

The dynamic equation for the heat flux is

$$(C-D)\overline{u_i\theta} = -\overline{u_iu_j}\frac{\partial T}{\partial x_j} - \overline{u_j\theta}\frac{\partial U_i}{\partial x_j} - \beta g_i\overline{\theta^2} - C_{1t}\frac{\epsilon}{k}\overline{u_i\theta} + C_{2t}\,\overline{u_j\theta}\frac{\partial U_i}{\partial x_j} - \frac{1}{5}\overline{u_j\theta}\frac{\partial U_j}{\partial x_i} + C_{3t}\beta g_i\overline{\theta^2} \tag{13}$$

where the first line on the right side is the production and the second line is the closure for $p\partial t/\partial x_i/\rho$. Neglecting convection and diffusion ($C - D = 0$) and the third term in the second line, equation (13) becomes

$$\overline{u_i\theta} = \frac{1}{C_{1t}}\frac{k}{\epsilon}\left[-\overline{u_iu_j}\frac{\partial T}{\partial x_j} - (1-C_{2t})\overline{u_j\theta}\frac{\partial U_i}{\partial x_j} - (1-C_{3t})\beta g_i\overline{\theta^2}\right] \tag{14}$$

where $C_{1t} = 3.0$, $C_{2t} = 0.5$, and $C_{3t} = 0.5$. Zeman and Lumley (1976) show that $C_{2t} = 0.8$ and $C_{3t} = 0.2$ from theoretical considerations.

Neglecting the convection and diffusional transport in equation (5) and eliminating ϵ_t with equation (6) gives

$$\overline{\theta^2} = -R\frac{k}{\epsilon}\overline{u_j\theta}\frac{\partial T}{\partial x_j} \tag{15}$$

which was given by Launder (1975, 1978) and used by Hossain and Rodi (1982).

Chen and Rodi (1975) and Chen and Chen (1979) used the differential equation (5), with ϵ_t eliminated by using equation (6) to determine $\overline{t^2}$ rather than using equation (15). In either case R is taken to be a constant equal to 0.8 (Hossain and Rodi, 1982; Chen and Rodi, 1975; Chen and Chen, 1979; Launder, 1975, 1978). It is seen in Fig. 2 that the experimentally determined value of R is much lower with an average value across the profile of roughly 0.25. Launder (1978) cites experimental evidence for R being in the range of 0.5 to 0.8. However, he found that the algebraic stress relations agreed best with an experiment for a stably stratified homogeneous shear flow with $R = 0.8$. Hence, that value has been adopted in the algebraic stress models. The experimental results of Shabbir and George (1987) indicate R is much lower for strongly buoyant flows. When the algebraic stress model is applied to this experiment with $R = 0.8$, the results are very poor for $\overline{t^2}$. Therefore, in the following evaluation of the algebraic stress model, the experimentally determined profile for R (Fig. 2) is used.

Equations (10), (12), and (13) represent a system of *algebraic equations* that can be solved for $\overline{u_i u_j}$, $\overline{u_i t}$, and $\overline{t^2}$. Employing the thin shear layer approximation, where only gradients in the radial direction are retained, Hossain and Rodi (1982) give

$$\overline{u^2} = \frac{2}{3}\frac{C_1 + C_2 - 1}{C_1} k + \frac{1 - C_2}{C_1}\frac{k}{\epsilon}\left(-2\overline{uv}\frac{\partial U}{\partial r} + 2\beta g \overline{vt}\right) \quad (16)$$

$$\overline{uv} = \frac{1 - C_2}{C_1}\frac{k}{\epsilon}\left(-\overline{v^2}\frac{\partial U}{\partial r} + g\beta\overline{vt}\right) \quad (17)$$

$$\overline{v^2} = \frac{2}{3}\frac{C_2 + C_2 - 1}{C_1} k \quad (18)$$

$$\overline{ut} = \frac{1}{C_{1t}}\frac{k}{\epsilon}\left[-\overline{uv}\frac{\partial T}{\partial r} - (1 - C_{2t})\overline{vt}\frac{\partial U}{\partial r} + (1 - C_{3t})\beta g \overline{t^2}\right] \quad (19)$$

$$\overline{vt} = \frac{-1}{C_{1t}}\frac{k}{\epsilon}\overline{v^2}\frac{\partial T}{\partial r} \quad (20)$$

$$\overline{t^2} = -2R\frac{k}{\epsilon}\overline{vt}\frac{\partial T}{\partial r} \quad (21)$$

from which $\nu_t = C_\mu k^2/\epsilon$ where

$$C_\mu = \frac{2}{3}\frac{(1 - C_2)(C_1 + C_2 - 1)}{C_1^2}\left(1 + \frac{1}{C_{1t}}\frac{k}{\epsilon} g\beta \frac{\partial T/\partial r}{\partial U/\partial r}\right) \quad (22)$$

The system of equations (16)–(21) was solved to determine the Reynolds stress and heat flux components with U, T, k, ϵ, and R given by the experiment. The following values for the constants were used:

$$C_1 = 2.2, \quad C_2 = 0.6, \quad C_3 = 0.6$$
$$C_{1t} = 3.0, \quad C_{2t} = 0.5, \quad C_{3t} = 0.5$$

The value of C_μ, which appears in the eddy viscosity relation $\nu_t = C_\mu k^2/\epsilon$ and is given by equation (22), is roughly 0.125 and is reasonably constant across the flow. This value is considerably larger than the value of $C_\mu = 0.09$ in the standard k–ϵ model. Rodi (1972), to correct for the discrepancies in the prediction for the axisymmetric jet, developed an empirical correction to C_μ. The parameter C_μ is replaced by $(1 - 0.465H)C_\mu$ where $H = 1(y_E/U_m)dU_m/dx|^{0.2}$. U_m is the maximum velocity, and y_E is the distance from the centerline of the edge of the jet. Hossain and Rodi (1982), Chen and Rodi (1975), and Chen and Chen (1979) used this correction in their predictions for turbulent buoyant jets. When the correction is applied, we get approximately 0.09, which is the value of C_μ for the standard k–ϵ model.

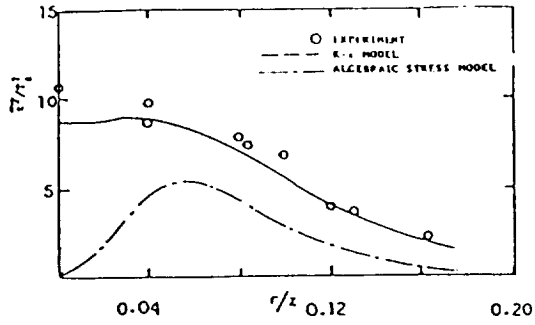

Fig. 7 Mean square temperature

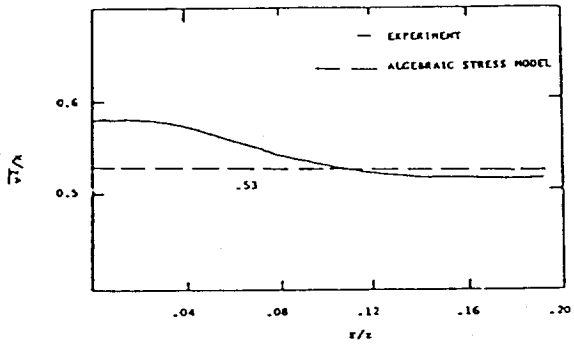

Fig. 8 Radial Reynolds stress $\overline{v^2}$

The question we are asking is, "given the turbulent energy, dissipation, velocity, and temperature, does the proposed algebraic stress expression correctly predict the Reynolds stress and heat flux components?" Figure 8 shows the radial Reynolds stress determined from equation (18). It is seen that the predicted value $\overline{v^2}/k = 0.53$ is a little smaller than the experimental curve in the center portion of the plume, but agrees quite well with experiment in the outer portion. The predicted shear stress $\overline{uv}$, the axial heat flux $\overline{ut}$, the radial heat flux $\overline{vt}$, and the mean squared temperature $\overline{t^2}$ are shown in Figs. 3, 4, 5, and 7, respectively. Again the points are experimental data and the broken lines are from the model. It is seen that the shear stress $\overline{uv}$ and radial heat flux $\overline{vt}$ are predicted reasonably. However, the vertical heat flux $\overline{ut}$ and temperature fluctuations $\overline{t^2}$ are predicted poorly and have incorrect shapes; unlike the experimental values they go to zero near the origin.

Equation (21) gives $\overline{t^2}$ proportional to the radial temperature gradient, which is zero at the centerline. Then since $\overline{t^2} = 0$ at $r = 0$, equation (19) gives $\overline{ut} = 0$ at $r = 0$. In order to obtain nonzero values for $\overline{ut}$ and $\overline{t^2}$ at the centerline from the model equations (12), (14), and (15), terms containing the axial gradient, i.e., $\partial U/\partial z$ and $\partial T/\partial z$, were retained. These terms were added to equations (19) and (21) and the system of equations was solved again. Although the centerline values of $\overline{ut}$ and $\overline{t^2}$ were found to be nonzero, the predictions still decreased to relatively small values near the centerline.

Another possibility for this behavior is the neglect of advection and diffusion terms in the model. Gibson and Launder (1976) have proposed the following model for these terms:

$$(C - D)_{\overline{u_i u_j}} = \frac{\overline{u_i u_j}}{k}(P + G - \epsilon) \quad (23)$$

$$(C - D)_{\overline{u_i t}} = \frac{\overline{u_i t}}{2\overline{t^2}}(P_t - \epsilon_t) + \frac{\overline{u_i t}}{2k}(P + G - \epsilon) \quad (24)$$

where P_t is the production term in the $\overline{t^2}$ equation. These were

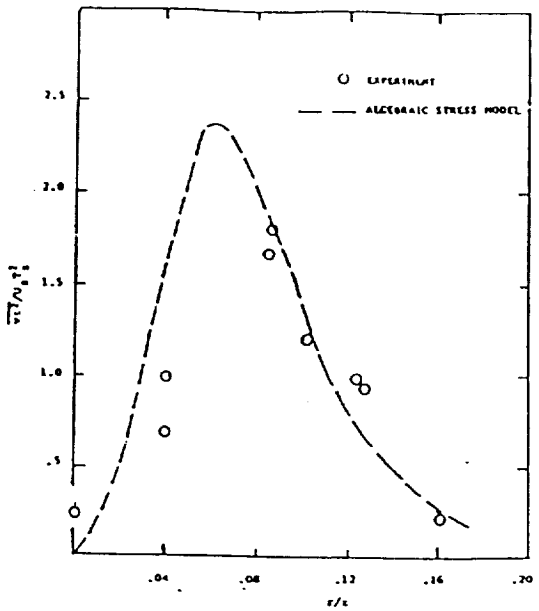

Fig. 9 Transport of temperature variance $\overline{t^2}$

incorporated in equations (16)–(21) and the resulting set of nonlinear coupled algebraic equations was solved simultaneously. The results did improve the prediction for the vertical heat flux $\overline{ut}$ and temperature variance $\overline{t^2}$ but the comparison for radial heat flux and shear stress became worse. As noted by Gibson and Launder (1976), the above model is not good near an axis of symmetry. This is why, by incorporating them in the original model, no overall improvement in the prediction is achieved.

Chen and Rodi (1975), Tamanini (1978), and Chen and Chen (1979) use the differential convective-transport equation (5) to determine $\overline{t^2}$ in their predictions of buoyant jets. Equation (6) was used to eliminate ϵ_t. Thus, the final form of the $\overline{t^2}$ equation becomes

$$U\frac{\partial \overline{t^2}}{\partial z} + V\frac{\partial \overline{t^2}}{\partial r} = \frac{1}{r}\frac{\partial}{\partial r}\left(C_t \frac{k^2}{\epsilon}\frac{\partial \overline{t^2}}{\partial r}\right) - 2\overline{vt}\frac{\partial T}{\partial r} - \frac{1}{R}\frac{\epsilon}{k}\overline{t^2} \quad (25)$$

This equation was numerically solved for the temperature variance $\overline{t^2}$ with all other quantities needed to evaluate the coefficients determined from experiments. The value of C_t was taken as 0.13. The best agreement, as shown in Fig. 7, was achieved with $R = 0.35$. When the average experimental value of $R = 0.25$ is used, the prediction peaks at about 6.0 ($\eta = 0.04$) as compared to the experimental value of $\overline{t^2}$ of about 8.0 ($\eta = 0.04$). When the standard value of $R = 0.8$ is used, $\overline{t^2}$ is overpredicted by a factor of four.

When $\overline{t^2}$ is calculated from the convective-transport equation (5), the diffusive transport is given by the simple gradient closure

$$\overline{vt^2} = -C_t \frac{k^2}{\epsilon}\frac{\partial \overline{t^2}}{\partial r} \quad (26)$$

with $C_t = 0.13$ as given by Chen and Rodi (1980). The prediction for $\overline{vt^2}$, using experimental information to evaluate the right-hand side of equation (26), is shown in Fig. 9. The predicted curve peaks somewhat above and toward the centerline as compared to the data.

Finally, we ask that if the models do not depict the axial heat flux $\overline{ut}$ and the temperature variance $\overline{t^2}$ correctly, then why do the predictions such as made by Hossain and Rodi (1982), Chen and Rodi (1975), Tamanini (1978), and Chen and Chen (1978) show reasonable agreement with the experiment for the mean velocity and buoyancy? The answer to this is that with $R = 0.8$ the temperature variance $\overline{t^2}$ from equation (21) or (25) is too large. This makes the vertical heat flux $\overline{ut}$ from equation (19) large enough so that the mean velocity and buoyancy are reasonably predicted.

5 Summary and Conclusions

The experimental data on buoyant plumes were used to evaluate various closure relations for turbulence transport. The objective was not to propose new models, but to evaluate the closure schemes proposed by other workers for buoyancy-dominated flows. The closures evaluated were those used in the k–ϵ and algebraic stress models. The results are summarized below.

1 The closure relations of the k–ϵ model compare reasonably with experimental data, except for the axial turbulent transport, which is drastically underpredicted. The axial heat flux governs the production due to buoyancy in the kinetic energy and dissipation equations and its correct prediction is very important. This is a probable reason why the results of Hossain and Rodi (1982) from the k–ϵ model underpredict the spreading rate for the plume by 10 percent even when axisymmetric jet corrections are included.

2 The ratio R of the time scales, which is used to determine the dissipation of the mean squared temperature in the algebraic stress model, was found to be considerably different from the accepted value of $R = 0.8$. Apparently R is not a universal constant, but can vary from flow to flow and is influenced by the strength of the buoyancy present. From the experimental data on a plume it appears that $R = 0.25$ for strongly buoyant flows.

3 The closure equations for the shear stress and radial heat flux of the algebraic stress models also compared well with experiment but are not better than the simple gradient closures used in the k–ϵ model. The axial heat flux and mean squared temperature are predicted poorly in the central core of the flow and had incorrect trends. This drawback could be attributed to the assumption of local equilibrium, which resulted in the neglect of convection and diffusion terms in the transport equations for Reynolds stress and heat flux. However, no substantial improvement was achieved by keeping the secondary derivatives or by incorporating the model for the convection and diffusion terms. Therefore, the full dynamic equations for Reynolds stress and heat flux with convection and diffusion are required to predict the axial heat flux and temperature variance properly.

Acknowledgments

This work was partially supported by the National Science Foundation under Grants ATM-8023699 and MSM 8316833.

References

Chen, C. J., and Chen, C. H., 1979, "On Prediction and Unified Correlation for Decay of Vertical Buoyant Jets," ASME JOURNAL OF HEAT TRANSFER, Vol. 101, pp. 532–437.

Chen, J. C., and Rodi, W., 1975, "A Mathematical Model for Stratified Turbulent Flows and Its Application to Buoyant Jets," *Proc. 16th Congress, IAHR*, Sao Paulo, Brazil, pp. 31–37.

George, W. K., Alpert, R. L., and Tamanini, F., 1977, "Turbulence Measurements in an Axisymmetric Buoyant Plume," *Int. J. Heat Mass Transfer*, Vol. 20, pp. 1145–1154.

Gibson, M. M., and Launder, B. E., 1976, "On the Calculation of Horizontal Non-equilibrium Turbulent Shear Flows Under Gravitational Influence," ASME JOURNAL OF HEAT TRANSFER, Vol. 98, pp. 81–87.

Hanjalic, K., and Launder, B. E., 1980, "Sensitizing the Dissipation Equations to Irrotational Strains," ASME *Journal of Fluids Engineering*, Vol. 102, pp. 34–40.

Hossain, M. S., and Rodi, W., 1982, "A Turbulence Model for Buoyant Flows and Its Application to Buoyant Jets," *Turbulent Buoyant Jets and Plumes*, W. Rodi, ed., Pergamon, NY, pp. 121–178.

Launder, B. E., 1975, "On the Effects of a Gravitational Field on the Turbulent Transport of Heat and Momentum," *J. Fluid Mech.*, Vol. 67, pp. 569–590.

Launder, B. E., 1978, "Heat and Mass Transport," *Topics in Physics, Vol. 12: Turbulence*, Springer-Verlag, New York, pp. 231–287.

Launder, B. E., Morse, A. P., Rodi, W., and Spalding, D. B., 1972, "The Prediction of Free-Shear Flows—A Comparison of the Performance of Six Turbulence Models," *Proc. Langley Free Shear Flows Conf.*, Vol. 1, NASA SP 320.

Launder, B. E., Reese, G. J., and Rodi, W., 1975, "Progress in the Development of a Reynolds-Stress Turbulence Closure," *J. Fluid Mech.*, Vol. 68, pp. 537–566.

Launder, B. E., and Spalding, D. B., 1974, "The Numerical Computation of Turbulent Flow," *Comp. Meth. in Appl. Mech. and Engr.*, Vol. 3, p. 269.

Lumley, J. L., 1978, "Computational Modeling of Turbulent Flows," *Advances in Applied Mechanics*, Vol. 18, pp. 123–176.

Pope, S. B., 1978, "An Explanation of the Turbulent Round-Jet/Plane-Jet Anomaly," *AIAA J.*, Vol. 16, pp. 279–281.

Rodi, W., 1972, "The Prediction of Free Turbulent Boundary Layers by Use of a Two-Equation Model of Turbulence," Ph.D. Thesis, Univ. of London, United Kingdom.

Shabbir, A., 1987, "An Experimental Study of an Axisymmetric Turbulent Buoyant Plume and Evaluation of Closure Hypotheses," Ph.D. Dissertation, Univ. at Buffalo, SUNY.

Shabbir, A., and George, W. K., 1987, "Energy Balance Measurements in an Axisymmetric Buoyant Plume," *Sixth Symposium on Turbulent Shear Flows*, Toulouse, pp. 9-3-1 to 9-3-6 (also submitted to *J. Fluid Mech.*).

Tamanini, F., 1978, "The Effect of Buoyancy on the Turbulence Structure of Vertical Round Jets," ASME JOURNAL OF HEAT TRANSFER, Vol. 100, pp. 659–664.

Zeman, O., and Lumley, J. L., 1976, "Modeling Buoyancy Driven Mixed Layers," *J. Atm. Sci.*, Vol. 33, p. 1988.